Supplementary Information for

Impacts of aerosol-photolysis interaction and aerosol-radiation feedback on surface-layer ozone in North China during a multi-pollutant air pollution episode

Hao Yang[1], Lei Chen[1], Hong Liao[1], Jia Zhu[1], Wenjie Wang[2], Xin Li[2]

[1]Jiangsu Key Laboratory of Atmospheric Environment Monitoring and Pollution Control, Jiangsu Collaborative Innovation Center of Atmospheric Environment and Equipment Technology, School of Environmental Science and Engineering, Nanjing University of Information Science & Technology, Nanjing 210044, China

[2]State Joint Key Laboratory of Environmental Simulation and Pollution Control, College of Environmental Sciences and Engineering, Peking University, Beijing 100871, China

Correspondence: Lei Chen (chenlei@nuist.edu.cn) and Hong Liao (hongliao@nuist.edu.cn)

Table S1. Locations of the three stations from NOAA's National Climatic Data Center used in this study.

Station	Latitude (°)	Longitude (°)
Beijing	40.08	116.585
Tianjin	39.1	117.167
Baoding	38.733	115.483

Table S2. Locations of the thirty-two stations from China National Environmental Monitoring Center used in this study.

Station	Latitude (°)	Longitude (°)
Beijing_1	39.8673	116.366
Beijing_2	40.2865	116.17
Beijing_3	39.9522	116.434
Beijing_4	39.8745	116.434
Beijing_5	39.9716	116.473
Beijing_6	39.9425	116.361
Beijing_7	39.9934	116.315
Beijing_8	40.1438	116.72
Beijing_9	40.3937	116.644
Beijing_10	40.1952	116.23
Beijing_11	40.0031	116.407
Beijing_12	39.9279	116.225
Tianjin_1	39.097	117.151
Tianjin_2	39.173	117.193
Tianjin_3	39.1654	117.145
Tianjin_4	39.1205	117.184
Tianjin_5	39.1082	117.237
Tianjin_6	39.0927	117.202
Tianjin_7	39.2133	117.1837
Tianjin_8	39.1337	117.269
Tianjin_9	39.0877	117.307
Tianjin_10	39.0343	117.707
Tianjin_11	38.8394	117.457
Tianjin_12	39.124	117.401
Tianjin_13	39.1587	117.764
Tianjin_14	38.9194	117.157
Baoding_1	38.8632	115.493
Baoding_2	38.8957	115.5223
Baoding_3	38.9108	115.4713
Baoding_4	38.8416	115.4612
Baoding_5	38.8756	115.442
Baoding_6	38.8707	115.5214

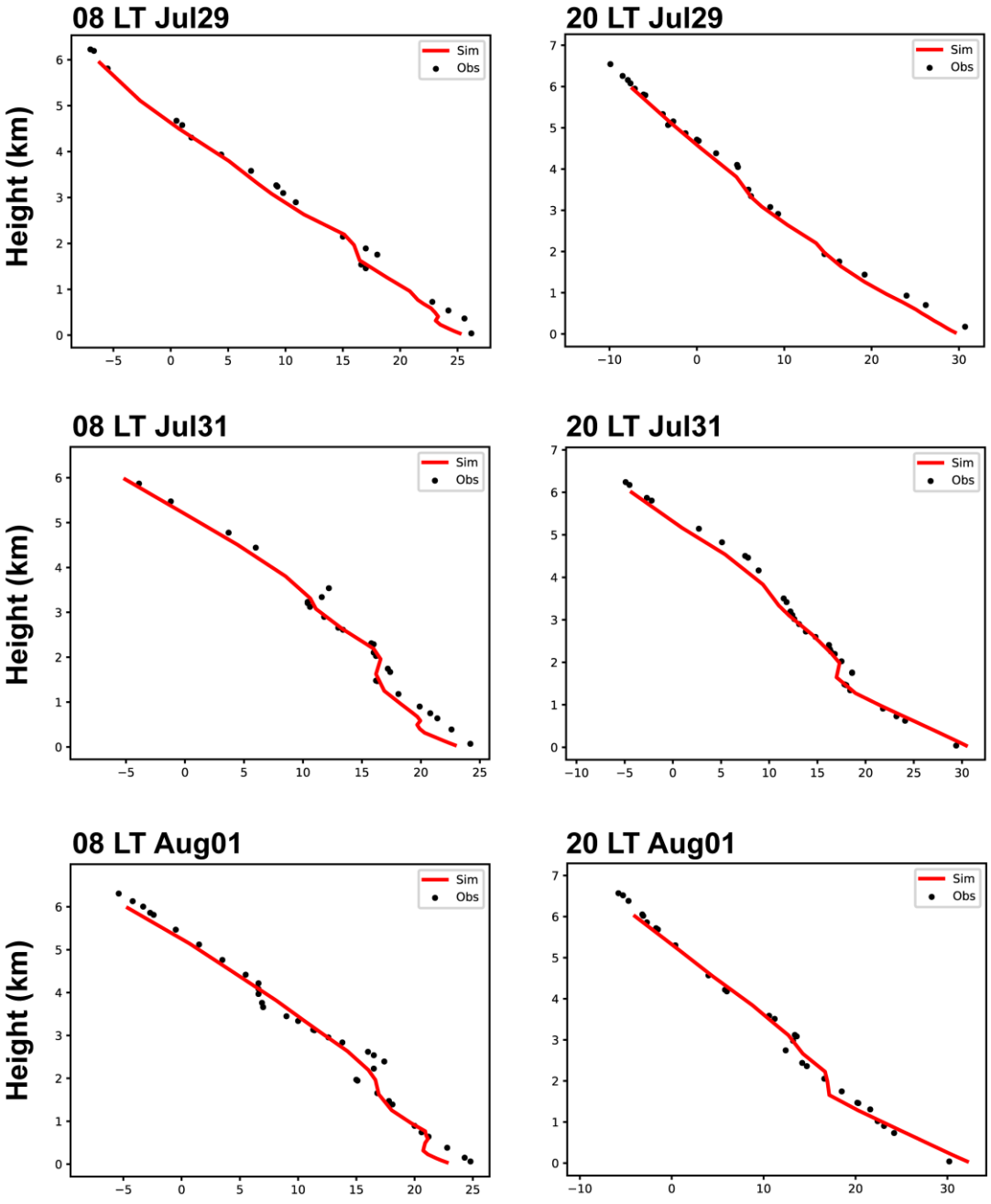

Figure S1. Observed (black dots) and simulated (red lines) temperature profiles in Beijing (39.93°N, 116.28°E) at 08:00 and 20:00 LST on 29 July, 31 July, and 1 August 2014.

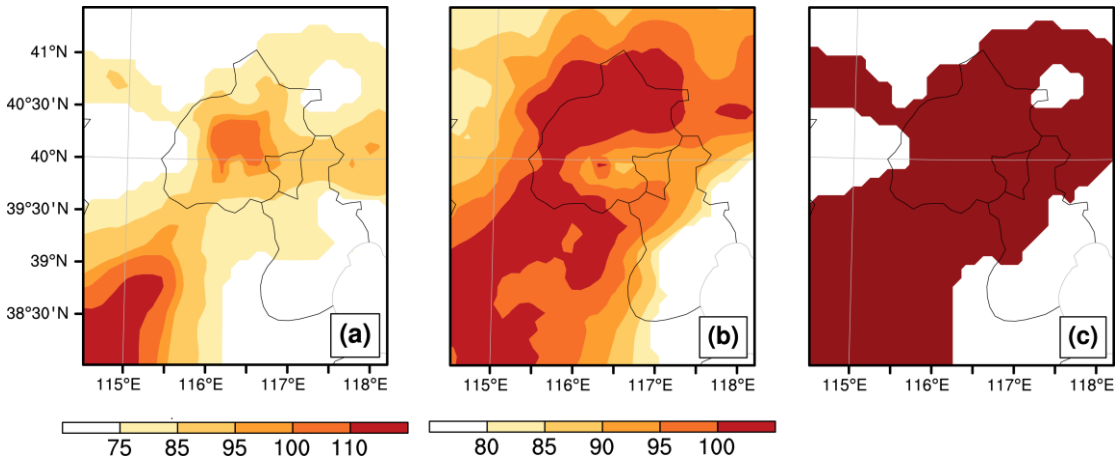

Figure S2. The spatial distributions of simulated (a) $PM_{2.5}$ (μg m^{-3}) and (b) MDA8 O_3 (ppb) concentrations averaged during 28 July to 3 August 2014. (c) The defined complex air pollution areas (CAPAs, shaded by red) where $PM_{2.5}$ and MDA8 O_3 concentrations are larger than 75 μg m^{-3} and 80 ppb, respectively.

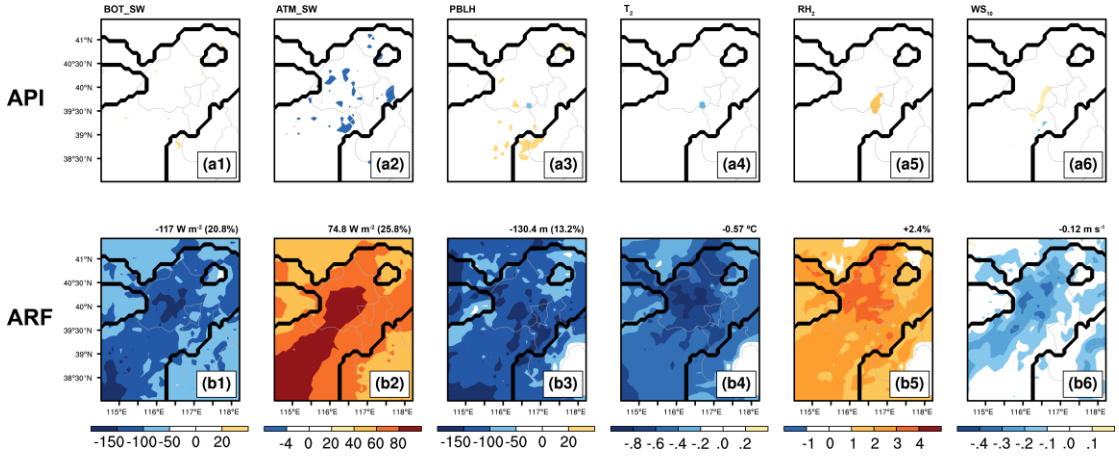

Figure S3. Changes in downward shortwave radiation at the surface (BOT_SW), downward shortwave radiation in the atmosphere (ATM_SW), PBL height (PBLH), 2-m temperature (T_2), 2-m relative humidity (RH_2), and 10-m wind speed (WS_{10}) caused by (a) API and (b) ARF during the daytime (08:00-17:00 LST) from 28 July to 3 August 2014. The calculated changes averaged over CAPAs are also shwon at the top of each panel.

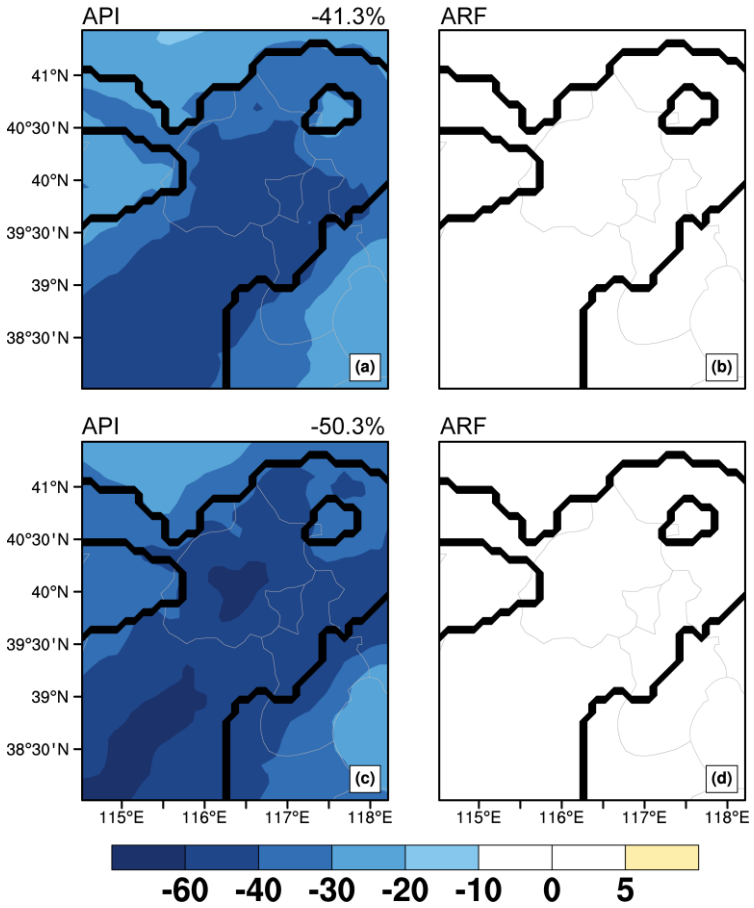

Figure S4. Percentage changes in (a-b) J[NO_2] and (c-d) J[O^1D] caused by API and ARF during the daytime (08:00-17:00 LST) from 28 July to 3 August 2014. The calculated changes averaged over CAPAs are also shwon at the top of each panel.

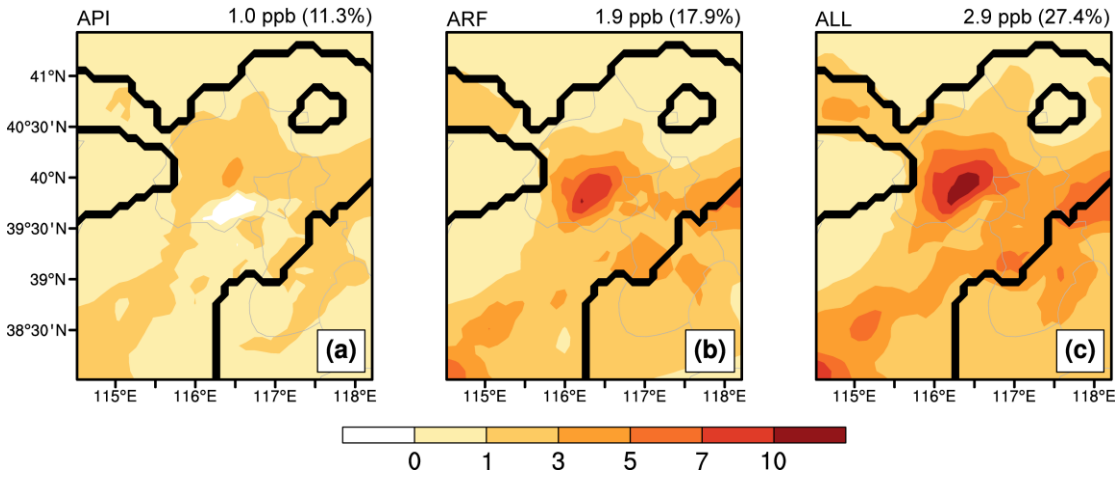

Figure S5. The changes in simulated surface-layer concentrations of NO_x (NO_2+NO, ppb) caused by (a) API, (b) ARF, and (c) ALL during the daytime (08:00-17:00 LST) from 28 July to 3 August 2014. The calculated changes averaged over CAPAs are also shwon at the top of each panel.

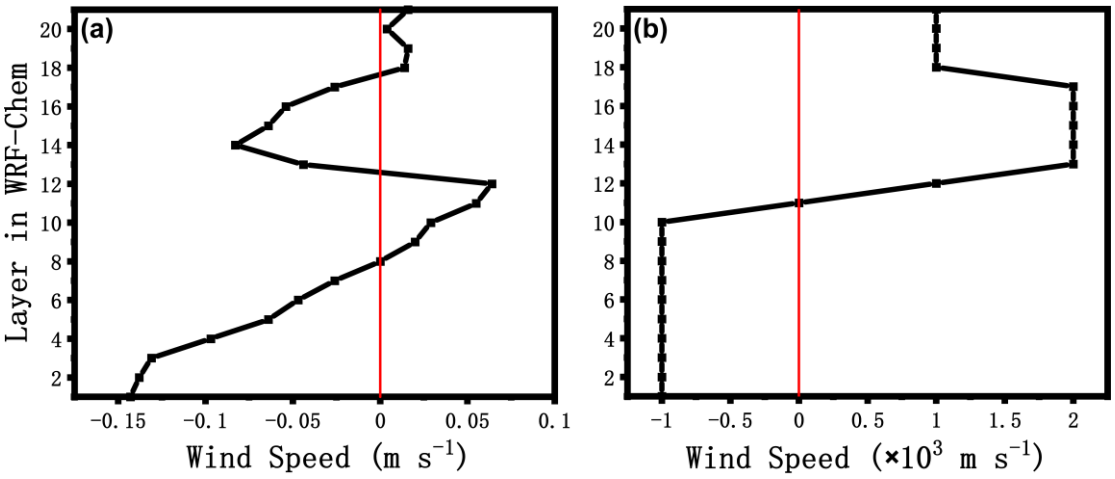

Figure S6. The impacts of ARF on (a) horizontal and (b) vertical wind speed in different model layers averaged over CAPAs during the daytime (08:00-17:00 LST) from 28 July to 3 August 2014.